2. SYNTHESIS OF TRIPLY LABELED TAXOL ANALOG FOR REDOR NMR STUDIES

2.1 Background

REDOR (Rotational–echo Double Resonance) NMR is a solid–state–NMR–spectroscopic tool to solve structures of biological macromolecules, such as proteins and enzyme–bound substrates by providing accurate internuclear distances. The method is useful in cases where X–ray and neutron diffraction methods fail to give the necessary resolution and in cases where the sample crystallizes poorly or not at all. REDOR NMR experiments are accomplished by specific stable isotope labeling of a ligand, and by subsequent measurement of the heteronuclear dipolar coupling between isolated pairs of labeled nuclei.[87]

NMR spectra of solutions usually have well resolved resonances because of fast tumbling of molecules. All interactions between the nuclei and the external magnetic field are anisotropic in nature. Fast tumbling of molecules leads to minimization (averaging) of anisotropy to isotropic values. However, NMR spectra of solids are broad and lack resolution due to multiple resonances induced by anisotropy a direct consequence of restricted motion of molecules in solids. Two interactions are important to address the issue of resolution of the NMR of solids, the dipolar interaction and chemical shielding anisotropy (CSA).

Dipolar interaction is an interaction between the magnetic moments of any nuclei with non–zero nuclear spin. Mathematically, for two nuclei with the same spin–state, the dipolar interaction is defined as:

$$H_d = C(1–3\cos^2\theta)/r^3$$

[87] a) Gullion, T.; Schaefer *J. Magn. Reson*. **1989**, *81*, 196.; b) Schaefer, J. In *REDOR NMR of Biological Solids From Protein Binding Sites to Bacterial Cell Walls: Recent Trends in Molecular Recognition*; Diedrich, F.; Künzer, H, Eds.; Ernst Schering Research Foundation: Workshop 26, 25–51.

where **r** is the internuclear distance, **C** is a constant and **q** is the angle between the internuclear vector and the direction of the applied magnetic field. In solutions with molecules tumbling fast the angular term averages to zero, hence dipolar interactions are not observed in solutions. In solids, a given nucleus experiences several dipolar interactions from neighboring nuclei, resulting in a variety of internuclear vectors and overlapping resonances ($\theta \neq 0$), causing a broad featureless signal.

In order to address the problem of chemical shift anisotropy and gain chemical shift resolution, a high–speed rotation of a sample at an axis tilted with a magic angle of 57.4^{o} (Magic Angle Spinning, MAS, derived from the above equation) relative to the applied field is used. Strategic stable isotope labeling is also done on the sample and allows the measurement of through–space dipolar coupling between two rare spins S (sensitive) and I (insensitive) (for example ^{13}C and ^{15}N).

Dipolar interactions between two spins depend on spatial orientation of the internuclear vector relative to the applied field, internuclear distance, and on the magnetic coupling of the two nuclei. Magic–angle sample spinning contributes to the averaging of the dipolar interaction over the spatial coordinate, while rotor synchronized radio–frequency pulses exclusively average out the spin coordinate. Both spin and space averaging processes are coherent and are of comparable frequency; hence their mixing leads to a constructive interference of averaging or recoupling. The degree of interference is a measure of dipolar coupling, which ultimately is related to the internuclear distance.

To suppress the unwanted multiples of dipolar coupling from the high abundance spins of ^{1}H, irradiation of the nuclei is performed during the entire evolution and acquisition period of the actual REDOR experiment. This procedure is similar to the conventional broad–band proton decoupling in ^{13}C NMR experiment, however, the instrumentation required to achieve the decoupling for solid state NMR experiments must have high power ranging between 100–200 watts.

A cross–polarization (CP) technique provides enhancement of signals from a less abundant but relatively sensitive nuclei S (^{13}C) through magnetization effects from the abundant proton nuclei (^{1}H) and faster rate of data accumulation due to reduced spin–

lattice relaxation times. Cross polarization can be achieved by a high–powered spin locking pulse during the preparation phase.[87b]

Rotational–echo double resonance (REDOR) is a dephasing experiment for pairs of unlike nuclei I and S, where recoupling of the heteronuclear spin interactions is measured. The actual REDOR experiment has two components; in the first part, a diminished signal S_o from the interfering pulses is detected from one of the nucleus. In the second part, the interfering pulses on the non–observed nucleus are omitted and a full echo signal S_o' is detected. Thus, the ratio $\Delta S/ S_o'$ (the REDOR difference is $\Delta S = S_o' - S_o$) is used as a direct measure of dipolar coupling between two nuclei which in turn gives us internuclear distance.[87b]

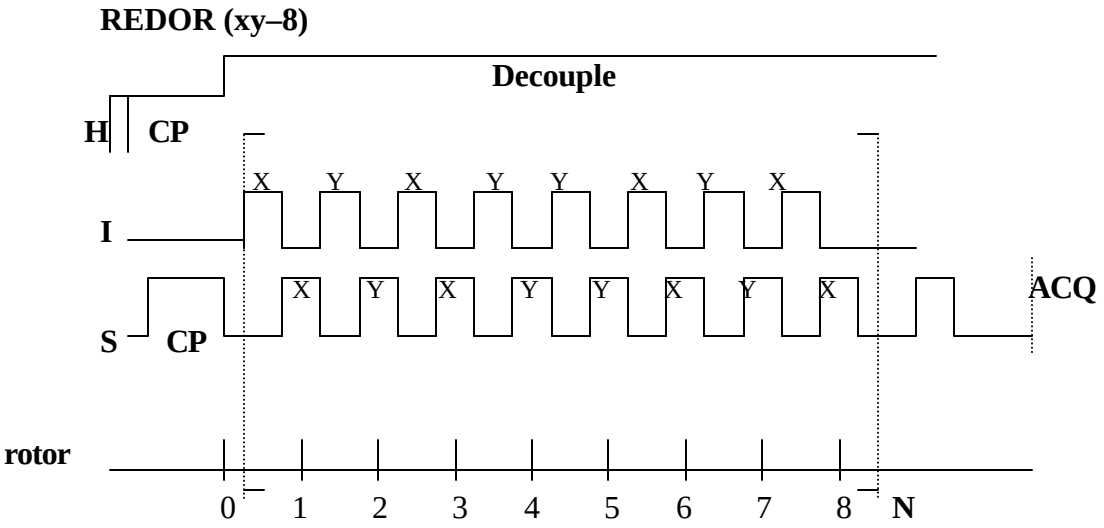

Figure 2.1 REDOR pulse sequence with π pulses on both the I and S channels.

2.2 REDOR Studies and Synthesis

Earlier REDOR studies of tubulin–bound taxol demonstrated the feasibility of the method to measure internuclear distances while taxol is bound on tubulin. The key experiment with the quadruply labeled analog **2.1** took a total of *three months* of acquisition time to obtain an acceptable signal–to–noise ratio. Distances between C–3' methine carbon and C–2 *p*–fluorobenzoate fluorine (9.8 ± 0.5 Å) and the carbonyl carbon of 3'–PhCONH and C–2 *p*–fluorobenzoate fluorine (10.3 ± 0.5 Å) were determined.[56]

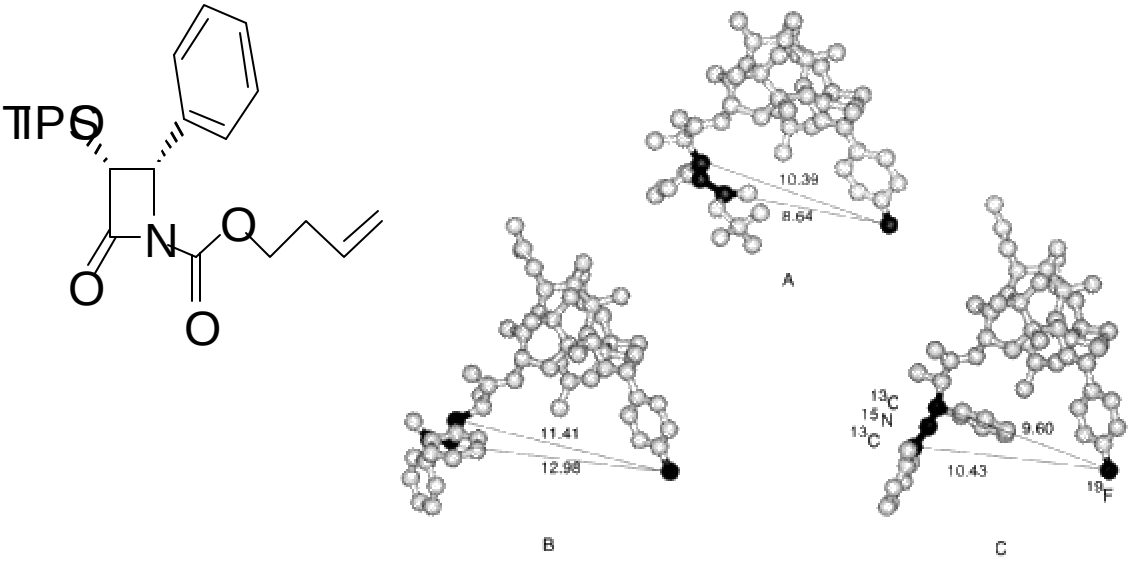

Figure 2.2 Possible conformation of microtubule–bound taxol. Structure **A** from X–ray coordinates of taxotere. Two different taxol conformations were found in the crystal corresponding to Structures **B** and **C** (Reprinted with permission from *Biochemistry*, **2000**, *39*, 281–291., Copyright 2000, American Chemical Society)

Comparison of these REDOR derived distances with three possible conformations of taxol shown in Figure 2.2, indicate that the values are close to conformations **A** (10.39 and 8.64 Å)[88] and **C** (10.43 and 9.60 Å)[89] but not conformation **B** (11.41 and 12.98 Å). Conformation **A** closely resembles the conformation of taxol in aprotic solvents while **C**

[88] The measured values in conformation **A** are for taxotere structure using X–ray coordinates (see ref. 80).
[89] Two different conformation (**B** and **C**) of taxol were found in the crystal. No solution conformation related to conformation **B** has been reported (see ref. 82).

resembles a conformation observed in protic solvents. Therefore, the results from the REDOR studies together with fluorescence spectroscopy showed good agreement with structure **A**, and help to rule out the less likely structure **B**, but are still inconclusive about structure **C**.

In order to acquire refined and unambiguous data, we initiated the synthesis of taxol analog **2.2** with a different pattern of labeling. In this analog, the triple labels were placed to reasonably represent the sidechain as well as all the southern regions of the baccatin skeleton. This pattern could allow us to determine distances between the deuterium atom on the sidechain phenyl group (D–Ph) and the fluorine atom on the C–2 benzoyl group, and simultaneously the distance between the fluorine atom and the C–4 deutroacetate group (CD_3CO).

The reterosynthetic analysis of compound **2.2** is given in Scheme 2.1. The major disconnection gave two main pieces for the synthesis; the baccatin core 2–debenzoyl–(2–*p*–fluorobenzoyl)–4–deacetyl–(4–d_3–acetyl)–7–triethylsilylbaccatin III (**2.3**) and (3*R*, 4*S*)–1–benzoyl–3–TIPSO–4–(*p*–deuterophenyl)azetidin–2–one **2.4**. The coupling of **2.3** and **2.4** was accomplished by Holton's protocol.

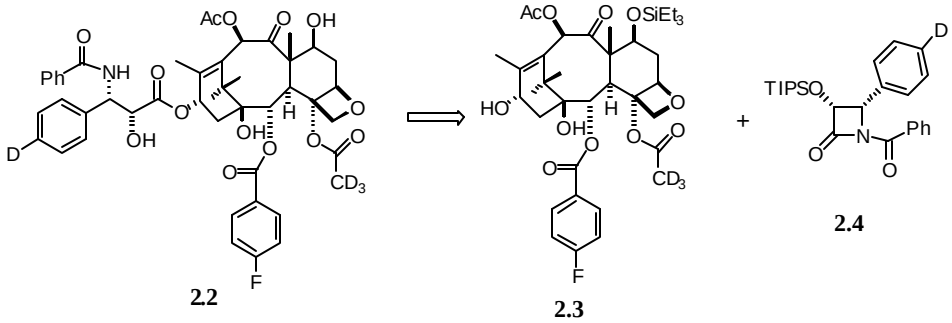

Scheme 2.1 Retrosynthetic analysis of labeled taxol analog

The forward synthesis sequence started from the natural product 10–deacetyl–baccatin (10–DAB, **2.5**) as shown in Scheme 2.2. Complete protection of the 7,10 and 13–hydroxyl groups was carried out, as initial acetylation of the 10–OH group was incompatible with the reaction sequence. The silyl protected baccatin core was treated with Red–Al® in THF to give a C–2 debenzoylated compound, which is weakly UV

absorbing.[90] Reesterfication of the C–2–hydroxy group was achieved with DCC/DMAP in dry toluene to give 4-fluorobenzoate **2.7** in 75% yield. Deacetylation of the 4-acetate group required prior protection of the hindered 1–OH position to block any neighboring group participation by coordinating to the Red–Al® reagent. Protection of the hindered 1–OH group was accomplished by the use of the less sterically demanding dimethylsilylchloride. Selective deacetylation of the C–4 acetate group was then achieved due to the coordination of the Red–Al® to the neighboring oxetane function. Reacetylation of the hindered hydroxyl group of DMS ether **2.8** using deuterated acetyl chloride gave the desired acetate **2.9** in 66% yield.[91] The low yield from the acetylation reaction is attributed to the loss of the dimethylsilyl protecting group on 1–OH and to incomplete conversion of the starting material even after prolonged reaction

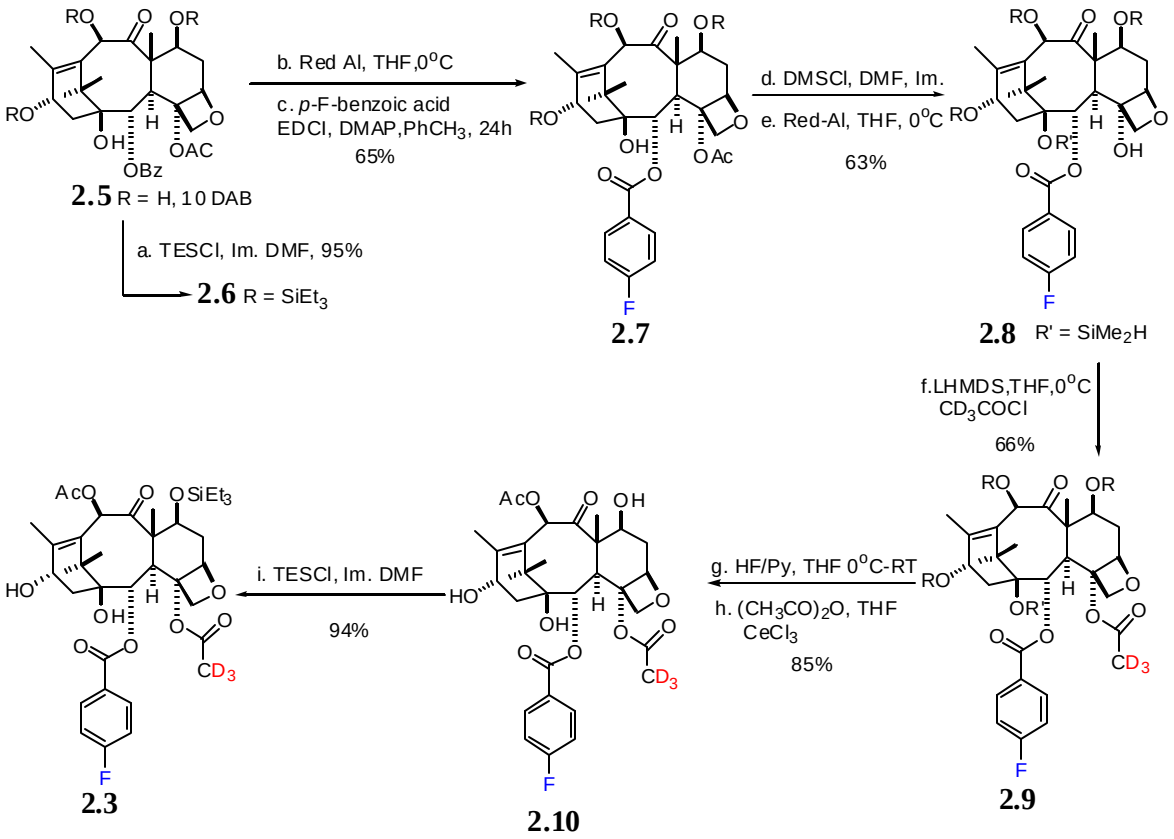

Scheme 2.2 Synthesis of the labeled baccatin core

[90] Karesenti–Marder, R.; Dubois, J.; Bricard, L.; Guenard, D.; Gueritte–Voegelein, F. *J. Org. Chem.* **1997**, *62*, 6631–6637

[91] Chen, S–H; Kadow, J. F.; Farina, V. *J. Org. Chem.* **1994**, *59*, 6156–6158.

period (72 hrs). Exhaustive deprotection of all the silyl groups was followed by selective acetylation[92] of the 10–OH mediated by $CeCl_3$ to give compound **2.10**. Selective reprotection of the 7–OH group completed the synthesis of the labeled baccatin core **2.3**.

The synthesis of the β–lactam sidechain started from commercially available 4–bromobenzaldehyde as shown in Scheme 2.3. Protection of the aldehyde function was followed by the deuterium exchange reaction. The protected deuterium–labeled aldehyde was then unmasked and reacted with *p*–anisidine to form the corresponding imine. Staudinger [2 + 2] cyclocondensation[93] of the imine with ketene generated from acetoxyacetyl chloride gave the racemic β–lactam **2.13** in 72% yield. Kinetic resolution of the racemic β–lactam[68j] with Lipase–PS–Amano enzyme gave two compounds, and the completion of the reaction was monitored by TLC. After chromatographic separation of the desired isomer (**2.14)**, deacetylation was carried out under basic conditions. Protection of the secondary alcohol as its triisopropylsilyl ether and Ce(IV)–mediated deprotection of the PMP group gave **2.15** in 70% yield. Benzoylation of **2.15** finally gave the desired labeled sidechain **2.4** in 87% yield.

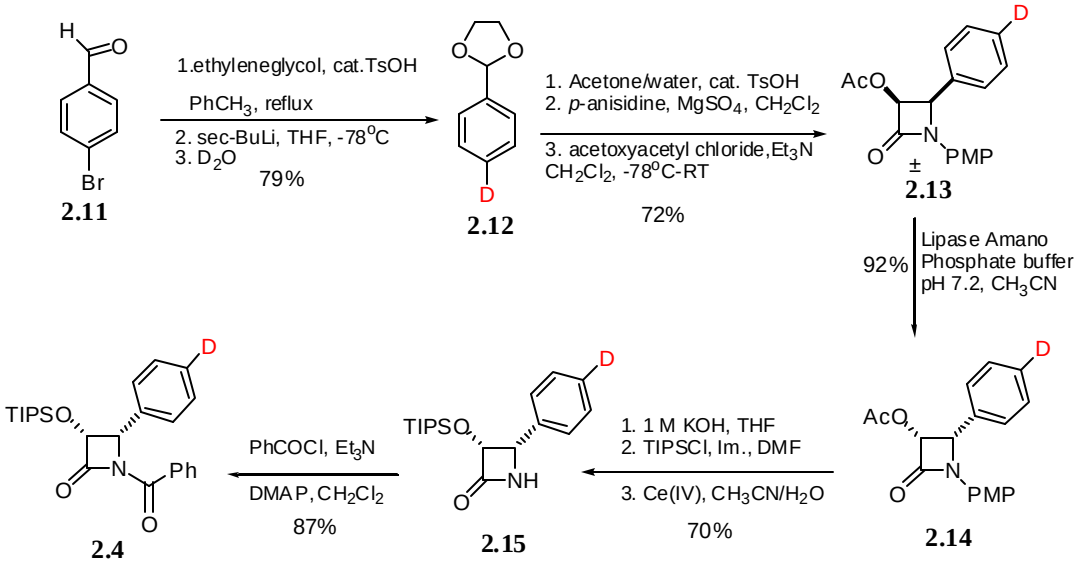

Scheme 2.3 Synthesis of deuterium labeled β-lactam

[92] Holton, R. A.; Zhang, Z.; Clarke, P. A.; Nadizadeh, H.; Procter, D. J. *Tetrahedron Lett.* **1998**, 2883–2886.
[93] Staudinger, H. *Justus Liebigs Ann. Chem.* **1907**, *356*, 51.

The synthesis of the target labeled taxol analog (**2.2**) was completed by a coupling reaction between the baccatin core (**2.3**) and β–lactam (**2.4**) and a deprotection step as shown in Scheme 2.4.

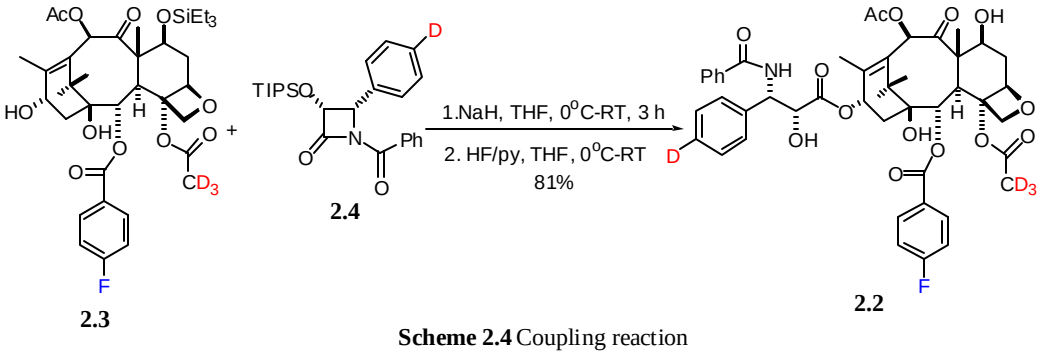

Scheme 2.4 Coupling reaction

The triply labeled analog was then submitted to our collaborators at SUNY in Binghamton for tubulin binding and shipped to Washington University in St. Louis for the REDOR NMR studies.

3. SYNTHESIS AND BIOLOGICAL EVALUATION OF NOVEL MACROCYCLIC TAXOL ANALOGUES

3.1 Background

The identification of the biologically relevant conformation of taxol while it is bound to tubulin is the key information needed to identify crucial interactions with the binding sites, and to extend this information to rationalize drug resistance as well as design the next generation of anticancer agents.

In a recent report, Snyder and co–workers proposed a T–taxol (butterfly) conformation of taxol based on the crystallographic electron density (Figure 3.1c) and chemical computations.[57] In this model, the C–2–benzoyl phenyl ring is positioned nearly equidistant from both the 3'–benzamide phenyl ring and the 3'–phenyl ring. The T–taxol conformation fits well with the electron crystallographic density of the computationally refined taxol–tubulin complex, and allows residue βHis^{229} to lie between the 3'–benzamide phenyl ring and the C–2–benzoyl phenyl ring. These workers also suggested that, the "hydrophobic collapsed" conformation cannot accommodate βHis^{229} as well as the T–taxol conformation does, and implied that the "hydrophobic collapsed" is a less likely conformation.[57]

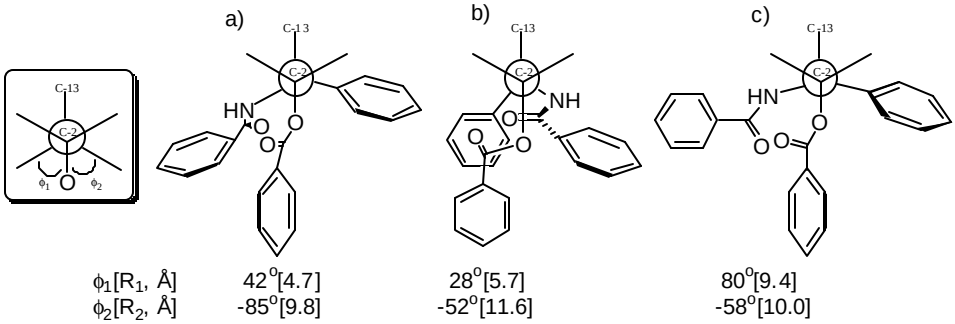

Figure 3.1 projections of taxol conformations; a) hydrphobic collapsed; b) extended; c) T– Newman taxol(butterfly)*

* Adapted from ref. 57.

In order to test the T–taxol hypothesis, and to examine the biological activity of conformationally defined taxol analogs, our group embarked on the synthesis of macrocyclic analogs tethered from the C–4 position to the sidechain by a linker. The design of this linker was suggested by molecular modeling studies, which indicated that it could mimic the T–taxol conformation.[94]

[94] Snyder, J. Personal communication.

3.2 Macrocyclic Taxol Analogs

The investigation of the conformation of taxol while it is bound to tubulin needs to be supported by data from the biological evaluation of taxol analogs with built–in conformational restrictions. A few reports with this primary goal have been published, including the synthesis of analogs with conformationally restricted side chains[95] and studies of analogs with bridges linking the C–3' and C–2 phenyls with both shorter[96] (**3.1**) and longer[86b] (**3.2**) linkers. Only the latter of the two bridged approaches yielded analogs with any activity, and this activity was significantly less than that of taxol even for the best analogs.

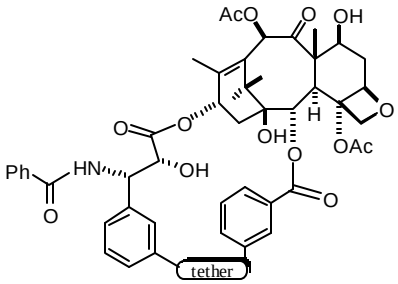

3.1

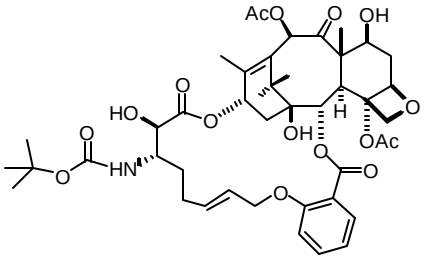

3.2

The T–taxol conformation sustains nearly 9–10 Å distance between the C–13 sidechain terminal phenyl rings and the C–2 benzoyl phenyl group. In this model, the C–4 acetate group is close to the 3'–phenyl group on the sidechain indicating conformational control between these groups. Hence, shorter linkers between these groups would not be the most likely targets; rather linkers that connect the C–4 acetate to the sidechain were envisioned to possess the T–taxol conformation.

In an attempt to model the T–taxol conformation, we initially designed and synthesized macrocyclic analogs **3.3** and **3.4** linked between the C–3'–phenyl group and the C–4 position.[97]

---

[95] Barboni, L.; Lambertucci, C.; Appendino, G.; Vander Velde, D. G.; Himes, R. H.; Bombardelli, E.; Wang, M.; Snyder, J. P. *J. Med. Chem.* **2001**, *44*, 1576–1587.
[96] Boge, T. C.; Wu, Z.–J.; Himes, R. H.; Vander Velde, D. G.; Georg, G. I. *Bioorg. & Med. Chem. Lett.* **1999**, *9*, 3047–3052.
[97] Metaferia, B. B.; Hoch, J.; Glass, T. E.; Bane, S. L.; Chatterjee, S. K.; Snyder, J. P.; Lakdawala, A.; Cornett, B.; Kingston, D. G. I. *Org. Lett*. **2001**, *3*, 2461-2464.

The synthesis of the macrocycles was first planned to be accomplished by Yamaguchi lactonization strategy, but the chemistry to attach the linker with its bulky protected carboxylic acid functionality at the C–4 position proved to be too difficult. The strategy was then changed, and the problem was addressed by employing a ring–closing olefin metathesis (RCM) method in the crucial macrocyclization step; this approach was selected because of recent precedent of its use in the taxol field and the wide scope of functional groups tolerated.[98]

The retrosynthetic analysis of macrocycles **3.3** and **3.4** is shown in Scheme 3.1. The

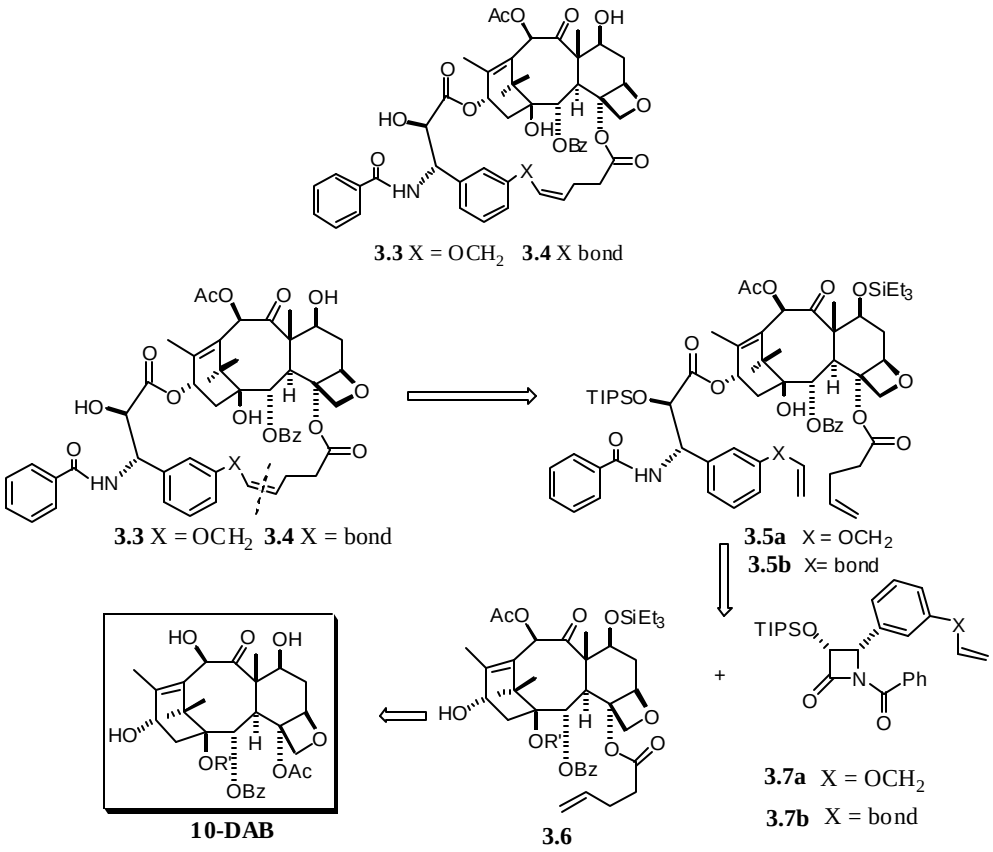

Scheme 3.1 Retrosynthetic analysis of macrocyclic taxol analogs

The synthesis of the key synthon **3.6** was achieved by the procedure of Scheme 3.2. The available starting material 10-deacetyl baccatin (**2.8**) was converted to the protected 4-deacetyl derivative **3.8** by a reported procedure.[91] Attempts to acylate the

[98] a) For a recent review on RCM see Furstner, A. *Angew. Chem. Int. Ed.* **2000**, *39*, 3012 –3043.; b) ref. 86b; c) Ojima, I.; Lin, S.; Inoue, T.; Miller, M. L.; Borella, C. P.; Geng, X.; Walsh, J. J. *J. Am. Chem. Soc.* **2000**, *122*, 5343–5353.

highly hindered C–4 hydroxy of **3.8** with 4–pentenoic acid and DCC/DMAP gave very low yields in several attempts under different reaction conditions. However, the use of 4–pentenoyl choride and LHMDS in THF at 0 ^{o}C gave the desired C–4 modified baccatin (**3.9**) in 78% yield. This reaction was accompanied by a minor C–4 acylated product which had also lost the dimethylsilyl group from the 1–OH position. The minor recovered material was used in the subsequent step.

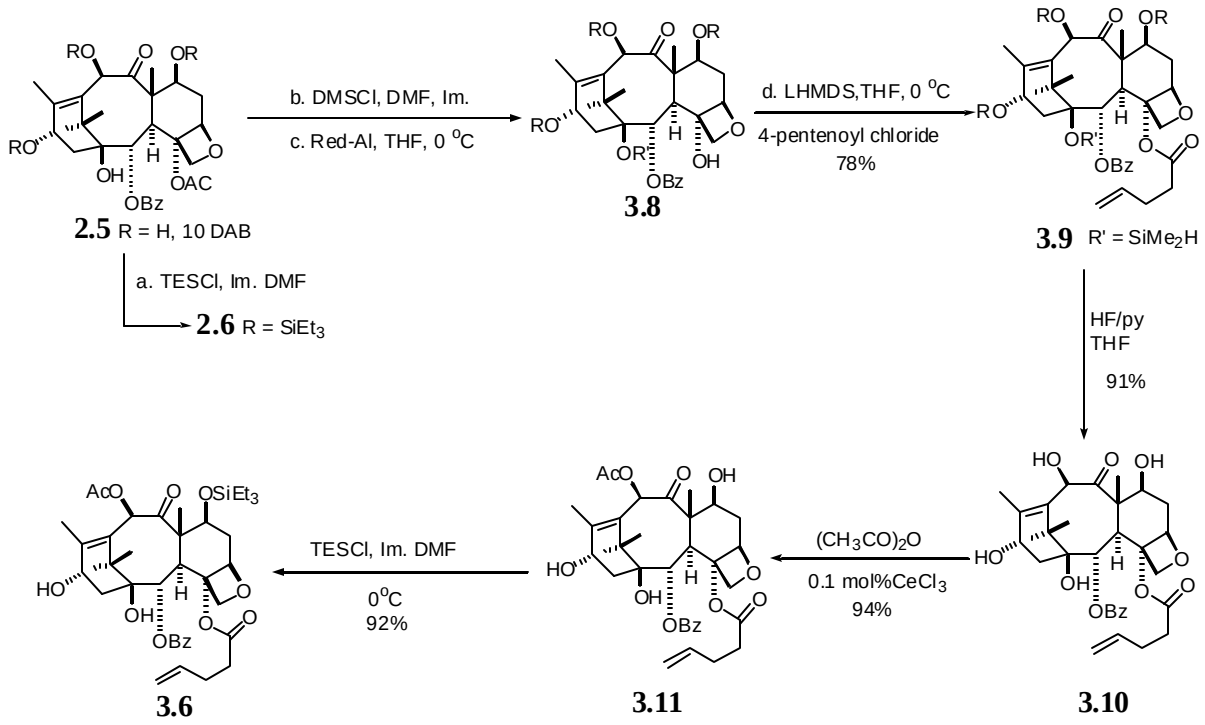

Scheme 3.2 Synthesis of the C-4 derivatized baccatin core

Exhaustive deprotection of the silyl groups using HF/pyridine to give **3.10** was followed by an efficient selective acetylation of the C–10 hydroxyl group mediated by a chelation effect of Ce(III) between the C–9 carbonyl function and the C–7 hydroxyl group.[92] The desired baccatin core **3.6** was secured after reprotection of the C–7 hydroxyl group as its triethysilyl ether in 92% yield.

The synthesis of (*3R,4S*)–1–benzoyl–3–TIPSO–4–(*m*–allyloxyphenyl)azetidin–2–one (**3.7a**) started from 3–allyloxybenzaldehyde (Scheme 3.3).[99] The aldehyde was reacted with *p*–anisidine to form the imine quantitatively. Cyclocondensation of the imine with a ketene generated from acetoxyacetyl chloride gave a racemic β–lactam. The lactam was then subjected to an enzymatic resolution using lipase to give compound **3.13** in 49% yield (98% yield based on the enantiomer present in the racemate). Basic hydrolysis of the acetate lactam followed by reprotection afforded the TIPS protected lactam in 94% yield. Oxidative deprotection of the PMP group with CAN then gave **3.14** in good yield. Benzoylation of **3.14** then gave the desired lactam **3.7a** in good yield.

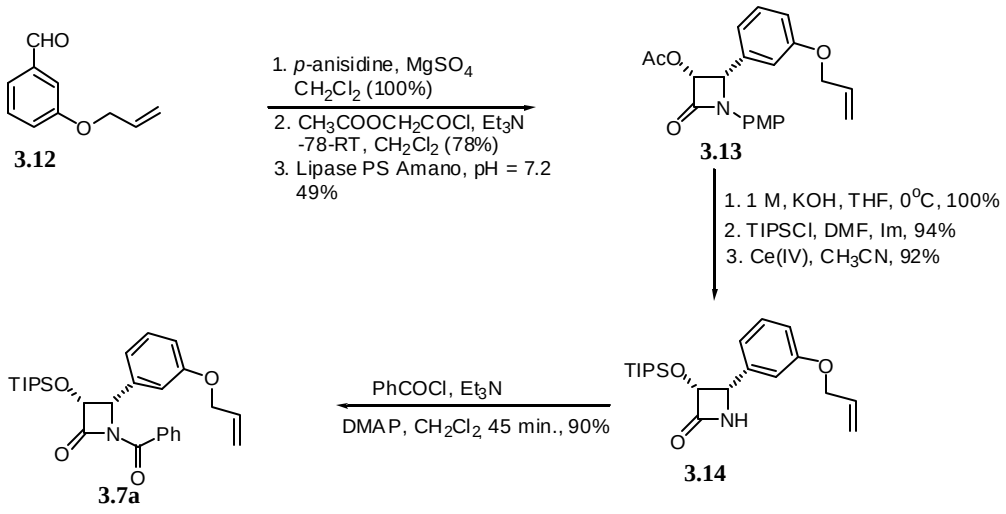

Scheme 3.3 Synthesis of β-lactam sidechain

The coupling reaction of the C–4 modified baccatin derivative **3.6** and β–lactam **3.7a** was carried out by employing the Holton–Ojima–Georg protocol[21c–d,65d] to yield

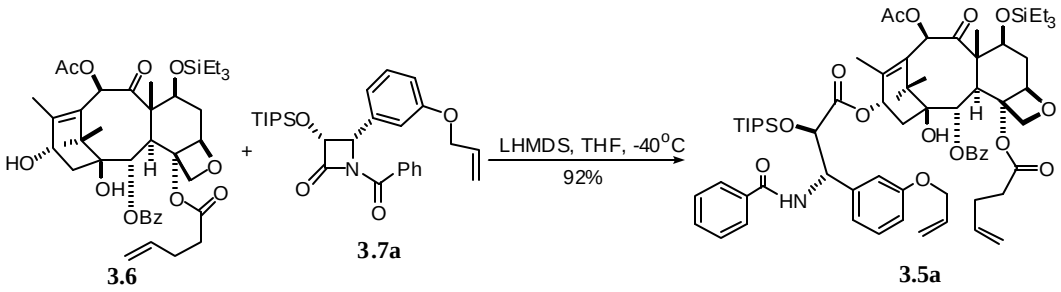

Scheme 3.4 Coupling reaction between C-4 modified baccatin with β-lactam

[99] Starting reagent **3.12** was synthesized from 3–hydroxybenzaldehyde and allylbromide.

taxoid–ù,ù′–diene **3.5a** (92%) (Scheme 3.4).

The crucial macrocyclization of taxoid–ù,ù′–diene **3.5** was performed using the first generation Grubbs catalyst [bis(tricyclohexylphosphine)benzylideneruthenium(IV) dichloride][100] in dichloromethane at room temperature and very slow addition via a syringe pump (Scheme 3.5). The reaction gave the protected 21–membered macrocyclic analog exclusively as the *Z*–isomer as determined by NMR in 72% yield. Removal of all the silyl protecting groups afforded the desired macrocycle analog **3.3**.

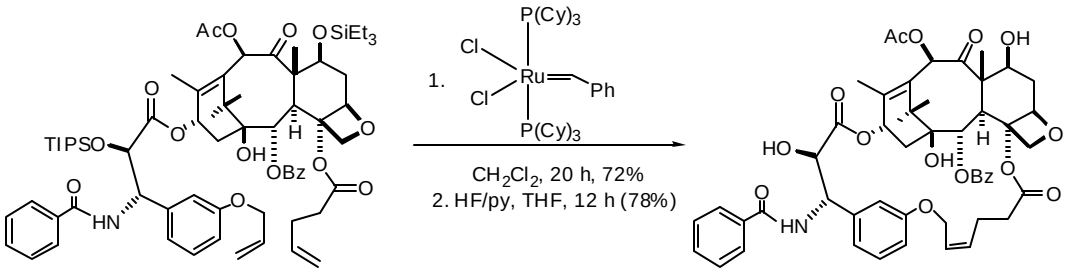

3.5a **3.3**

Scheme 3.5 Ring-closing olefin metathesis of taxoid-ω,ω'-diene

A similar sequence of reactions was followed to synthesize the macrocyclic analog **3.4** from the same baccatin derivative **3.6** and β–lactam **3.7b** as shown in Scheme

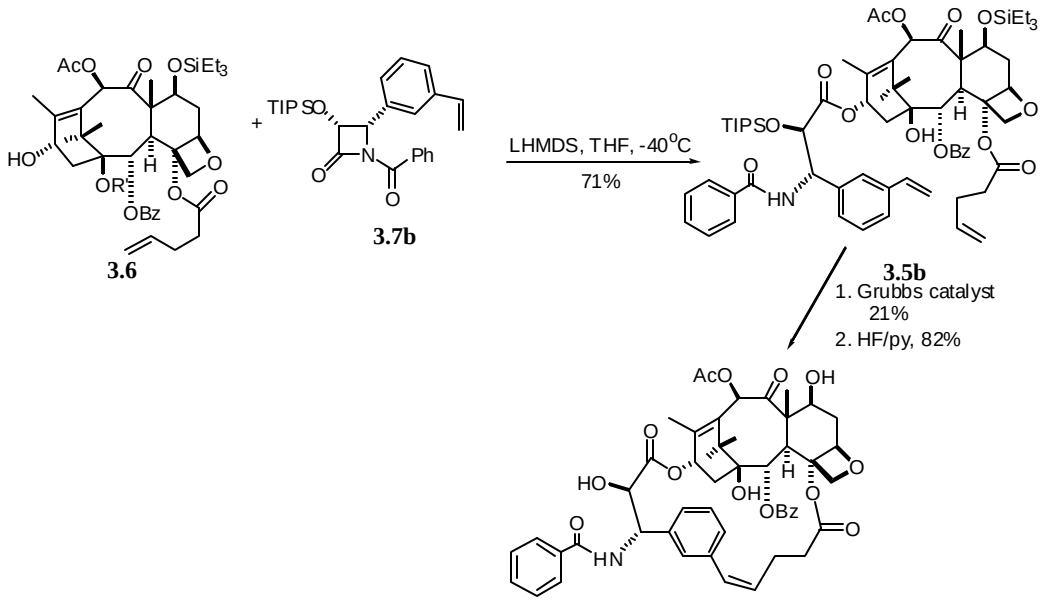

3.4

Scheme 3.6 Synthesis of macrocyclic taxol analog **3.4**

[100] Nguyen, S. T.; Grubbs, R. H.; Ziller, J. W. *J. Am. Chem. Soc*. **1993**, 115, 9856

3.6.

Bioassays of macrocyclic compounds **3.3** and **3.4** were performed with the A2780 (human ovarian cancer) mammalian cytotoxicity assay and a microtubule assembly assay. Compound **3.3** showed a tenfold decrease in activity compared to taxol in both cytotoxicity and microtubule assays (Table 3.1). Macrocyclic analog **3.4** showed about a 30–fold lesser activity. Comparison of these data with those obtained by Ojima et al., for macrocycles tethered from C–2 to the sidechain,[96c] shows that analogs **3.3** and **3.4** exhibited higher cytotoxicity values relative to taxol than those from Ojima's laboratories. However, in the microtubule assembly assay the activities for both macrocycles were not as high as of the best compounds obtained by Ojima.

Table 3.1 Bioactivity Results for Compounds **3.3** and **3.4**

Compound	Tubulin assembly Activity(I_{50}, mM)	Cytotoxicity to A2780 mammalian cells (IC_{50}, mg/mL)[a]
Taxol	0.27 ± 0.05	0.14 ± 0.08
3.3	2.54 ± 0.53	1.14 ± 0.03
3.4	8.10 ± 1.00	1.07 ± 0.05

[a]The strain A2780 used in these experiments consistently gave IC_{50} values in the range 0.06–0.15 mg/mL for taxol. These values are higher than those of other workers and are presumably due to variation in the strain used. The same strain was used for taxol and for compounds **3.3** and **3.4**.

The observed weaker activities led us to further investigate the possible conformations of these analogs. Our collaborators (Snyder and co–workers) performed a Monte Carlo conformational search on **3.3** and **3.4** with several force fields such as MM2*, MM3* and MMFF (GBSA/H_2O)[101] with 5 kcal/mol energy window produced a combined set of 500–1200 conformers. These conformers contain torsional isomers with excellent superposition of both the baccatin core and the C–2, C–4, and C–13 side chains on the same moities of T–taxol. So the underlying question was: *if the T–taxol is the bioactive conformation on β–tubulin and our model compounds possess this*

[101] Mohamadi, F.; Richards, N. G. J.; Guida, W. C.; Liscamp , R.; Lipton, M.; Caufield, C.; Chang, G.; Hendrickson, T.; Still, W. C.; *J. Comput. Chem.* **1990**, *11*, 440–449.

conformation why did we not get a comparable biological activity similar to taxol? One plausible reason would be that, the T-forms could be too high in energy. In order to test this hypothesis, we resorted to study the conformational profile of compound **3.3** in solution by NAMFIS (NMR Analysis of Molecular FlexIbility in Solution) analysis.[102]

Table 3.2 Distances calculated from 2D–ROESY for **3.3**.

Proton–proton(nOes)	Build–up Rate (γ_1, units/sec)	Distance calcd. r_1(Å)
H–13, Me–17	20.56	2.13
H–10, Me–18	26.45	2.04
H–3, H–10	5.70	2.64
H–7, H–10	21.83	2.11
H–2, Me–16	17.47	2.19
H–2, Me–19	12.59	2.31
H–2', H–3'	6.83	2.56
H5, H–6a	13.75	2.28
H–20a, Me–19	1.74	3.21
H–20b, Me–19	10.62	2.38
H–7, H–6a	14.10	2.27
H–3, H–7	15.57	2.23
H–6a, H–6b*	62.06* (γ_2*)	1.77* (r_2*)
H–3, Me–16	3.31	2.89
H–3, Me–19	2.71	2.98
H–3, Me–18	3.76	2.82
H–3, H14a,b	8.70	2.46
$OCH_2\alpha$, $OCH_2\beta$	23.8	2.08
H–5, H6b	3.45	2.87
H–2, H–7	3.05	2.92
O–Ph1, H–20b	1.10	3.47
O–Ph2, 3'NH	4.95	2.70
O–Ph3, H–2'	2.47	3.03
O–Ph3, OCH_2	3.66	2.84
O–Ph3, H–3'	8.72	2.46
O–Ph3, vinyl–Ha	3.17	2.91
O–Ph3, vinyl–Hb	2.48	3.03
O–Ph3, OCH_2	4.43	2.75
O–Ph1, H–20a	2.42	3.04

Our laboratories acquired a 2–D ROESY NMR data with mixing times of 70, 100, 150, and 180 ms for **3.3**. Careful integration of the nOe cross–peaks produced well defined volumes, which were then plotted against mixing times. From the linear region of the curves, slopes were calculated to give build–up rates (γ). Intermolecular distances

[102] Cicero, D. O.; Barbato, G.; Bazzo, R. *J. Am. Chem. Soc*. **1995**, *117*, 1027–1033.

(r) were then calculated under initial rate approximation condition (Table 3.2).[103] Together with intermolecular distances, the coupling constant *J*(H2'–H3') = 1.54 Hz was used in the NAMFIS analysis.

The NAMFIS analysis from Snyder's laboratories gave a total of eight conformers with predicted populations ranging from 2–35% (ΔΔG 0–1.7 kcal/mol); two nonpolar forms (40%) and extended conformers (60%, with 5% being the T–conformation) were identified. In this NAMFIS analysis, no polar forms of taxol were detected.

Docking of the T–conformers of **3.3** and **3.4,** derived from Monte Carlo search, into the taxol binding pocket of the refined electron crystallographic structure of β–tubulin showed that the bridged taxol analogs do not fit as well as T–taxol in the hydrophobic binding pocket. This result is consistent with the weaker activities observed for **3.3** and **3.4** (Figure 3.1).[104]

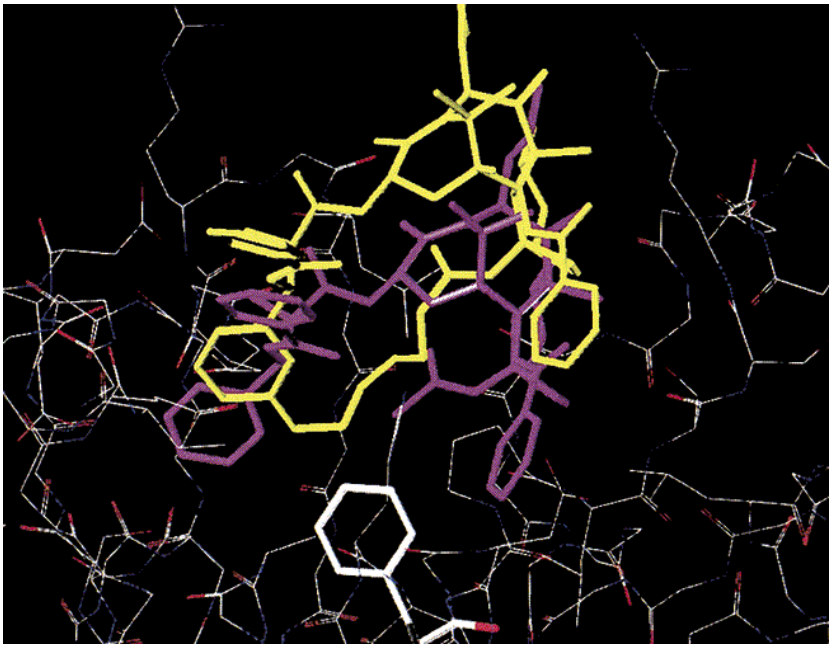

Figure 3.2 T–Taxol (magneta) bound to β–tubulin. The best T–form of compound **3.3** (yellow) is situated higher in the same pocket as a result of close contact between the tether and residue β^{Phe272} (white). (Reprinted with permission from *Org. Lett.* **2001**, *3*, 2461–2464. Copyright 2001, American Chemical Society)

---

[103] * reference distance and build up rate relationships $r_1/r_{2*} = (\gamma_{2*}/\gamma_1)^{-1/6}$
(This relationship holds true if nOe enhancements depend only on the cross–relaxation rate constants; This is called initial rate approaximation condition)

[104] NAMFIS analysis and docking experiments were performed by J. P. Snyder at Emory University

Macrocyclic analogs with linkers from the *o*–3'–phenyl group to the C–4 acetate group were also of interest in our investigation, because they would possibly have better binding to tubulin than the two analogs already discussed. The synthesis of these analogs was proposed based on the retrosynthesis analysis shown in Scheme 3.7.

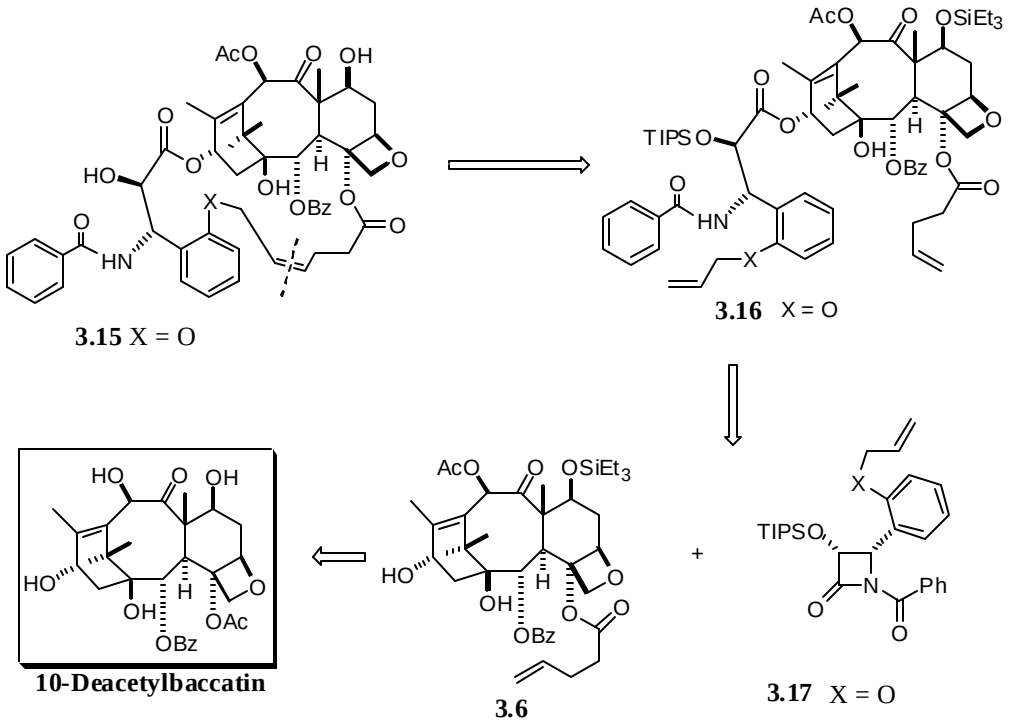

Scheme 3.7 Retrosynthetic analysis of macrocyclic taxol analogs

The synthesis of the requisite ring–closing reaction substrate **3.15** was accomplished by the coupling of **3.6** and **3.17** using a similar protocol to that previously described in Scheme 2.4. A total of sixteen steps was necessary to prepare this substrate.

Ring–closing reaction of **3.16** and **3.18** was attempted with Grubbs catalyst under various conditions, as well as with the second generation Grubbs catalyst [tricyclohexylphosphine(1,3–bis(2,4,6–trimethylphenyl)–4,5–dihydroimidazol–2–ylidene)(benzylidene)ruthenium(IV)dichloride][105] catalyst concentrations between 10 mol% and 50 mol%, dichloromethane, toluene and benzene as solvents, and various temperatures of reaction were investigated (Table 3.3). Unfortunately, in all of the

attempts the reaction gave only complex mixtures of polar products together with 20% of recovered starting material; no formation of the desired monocyclized product was observed.

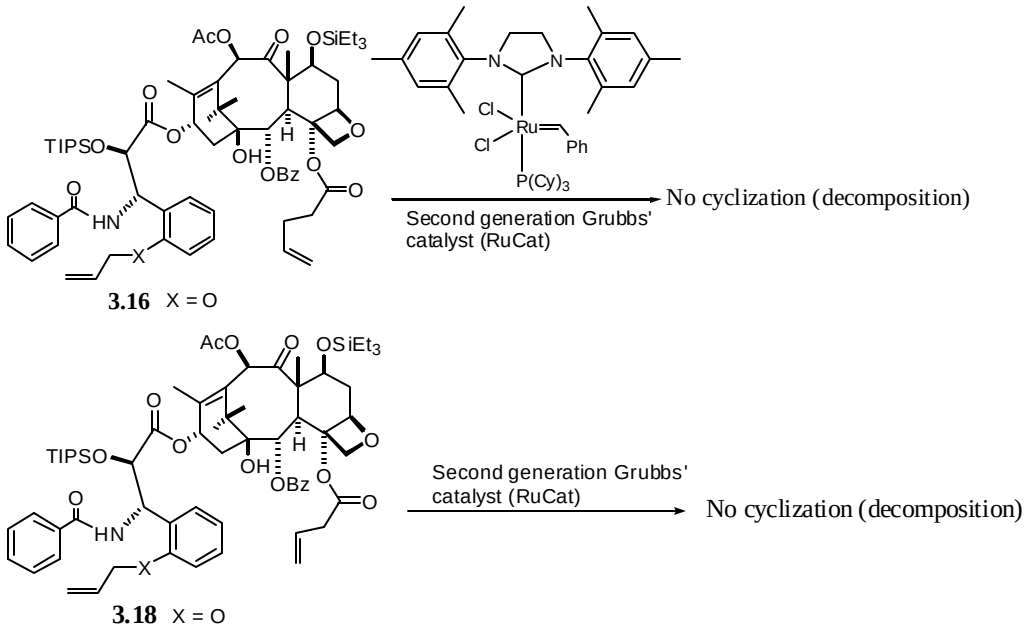

Scheme 3.18 Attempted macrocycization reactions

Table 3.3 Attempted olefin metathesis reaction conditions for **3.16** and **3.18**.

Variables	Conditions
Temperature	22–111 ^{o}C
Solvent	dichloromethane, toluene, benzene
mol %(RuCat.)	10–50
Rate of addition (RuCat.)	0.08–2 mL/min
Reaction time	1–4 days

The NMR spectra of the highly polar undesired reaction products showed in most of the cases no loss of the silyl protecting groups. The high polarity mixture was probably due to complexation of the ruthenium catalyst with the substrate without leading to productive cyclization. The chromatographic behaviors were not of homogenous compounds; they showed diffused and streaking bands in all of the cases.

[105] Scholl, M.; Ding, S.; Lee, C.W.; Grubbs, R. H. *Org. Lett*. **1999**, *1*, 953–956.

3.3 Discussion

The propene fragment on the C4–C3' tether (in compound **3.3**) has a close contact between residues β^{Ala233} and β^{Phe272} in floor of the cleft. Molecular dynamics studies on the complex of Figure 3.2 indicated that the interaction between β^{Phe272} and the tether remains to interfere with effective binding. Thus, while the present results are compatible with the T–taxol binding motif, they suggest that a flexible and extended bridge may not be the optimal design for full expression of taxoid activity.

The preparation of macrocyclic analogs with shorter linkers with a ring–closing olefin metathesis strategy posed difficulties at the crucial cyclization step of the synthesis. A possible alternate approach for future work would be to use the classical Yamaguchi macrolactonization. This would require that the terminal olefins of the substrates be transformed either to primary alcohols or to carboxylic acids without affecting the baccatin core.

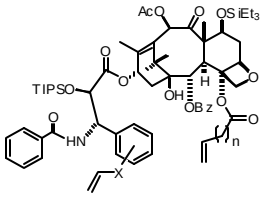

Table 3.4 Heat of reactions calculated for model macrocyclization reactions

Compound	X	*o/m*	n	Atoms in the linker(after cyclization)	ΔH kcal/mol (MMFF)	ΔH kcal/mol (AM1)	Cyclized Product (%)
A (**3.4**)	bond	*m*	2	4	–0.9	+ 1.0	21
B (**3.3**)	OCH_2	*m*	2	6	+6.3	+ 3.6	78
C	bond	*o*	1	3	+6.3	+ 2.8	0
D (**3.18**)	OCH_2	*o*	1	5	+9.3	ND	0
E (**3.16**)	OCH_2	*o*	2	6	+13.0	+ 7.1	0
F	OCH_2CH_2	*m*	2	7	+2.5	+ 4.0	*
G	OCH_2CH_2	*o*	2	7	+18.7	+1.0	*

*F and G were longer chain analogs considered only for the purpose of calculation, ND = not determined

Energy calculations (MMFF, AM1) for macrocyclization reaction of some of the target macrocyclic analogs were performed. The heat of reactions for all of the macrocyclic analogs were endothermic (by about 1 to 18 kcal/mol) and did not show any trend on the ease of macrocyclization (Table 3.4). The results of the calculations suggested that macrocyclization reactions probably were driven mainly by entropic factor. For compounds **3.3** and **3.4** the entropy effect must have offset the endothermicity and led to macrocyclization.

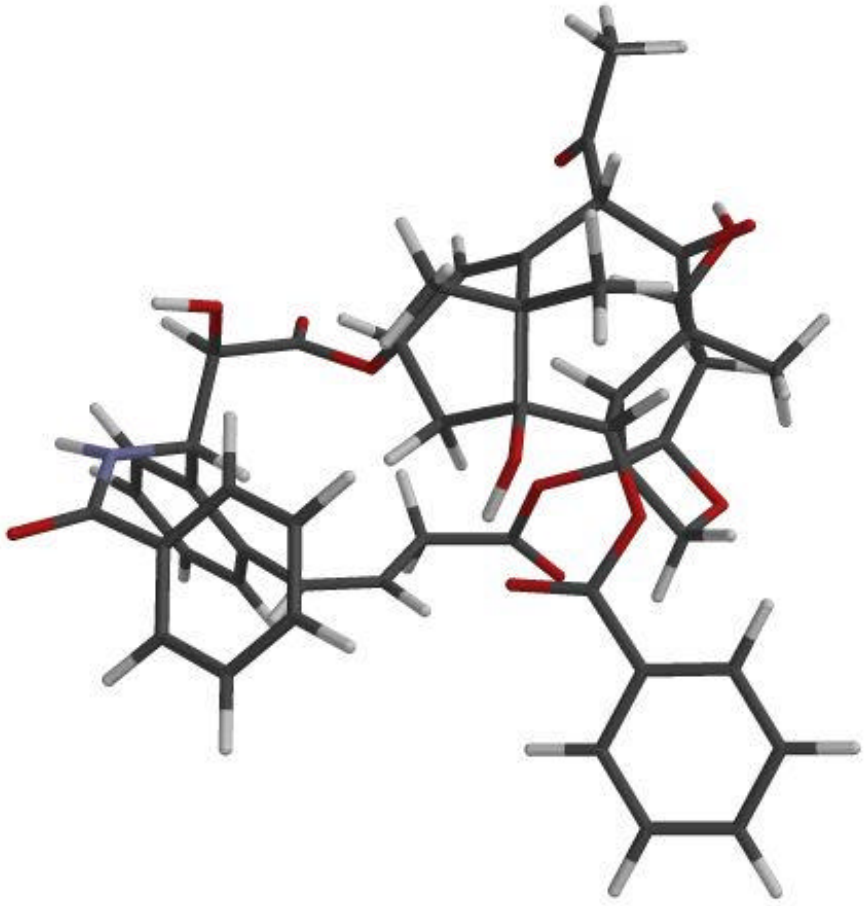

Figure 3.3 AM1 minimized macrocyclic analog C (ΔH = +2.8 kcal/mol)

4. SYNTHESIS OF MACROCYCLIC ANALOGS TETHERED FROM C–10 TO SIDECHAIN

4.1 Synthesis of C–10 Tethered Taxol Analogs

Previous SAR studies[65c] indicate that the northern hemisphere of taxol does not play a crucial role in the activity of taxol, since the C–10 acetate group can be removed or replaced by other groups without losing activity. Hence, we proposed that a linker between C–10 and the sidechain would introduce conformational control without adversely affecting the activity. From a synthetic point of view the "inverted cup" 3–D structure of taxol was anticipated to impose a synthetic challenge during the crucial macrocyclization step.

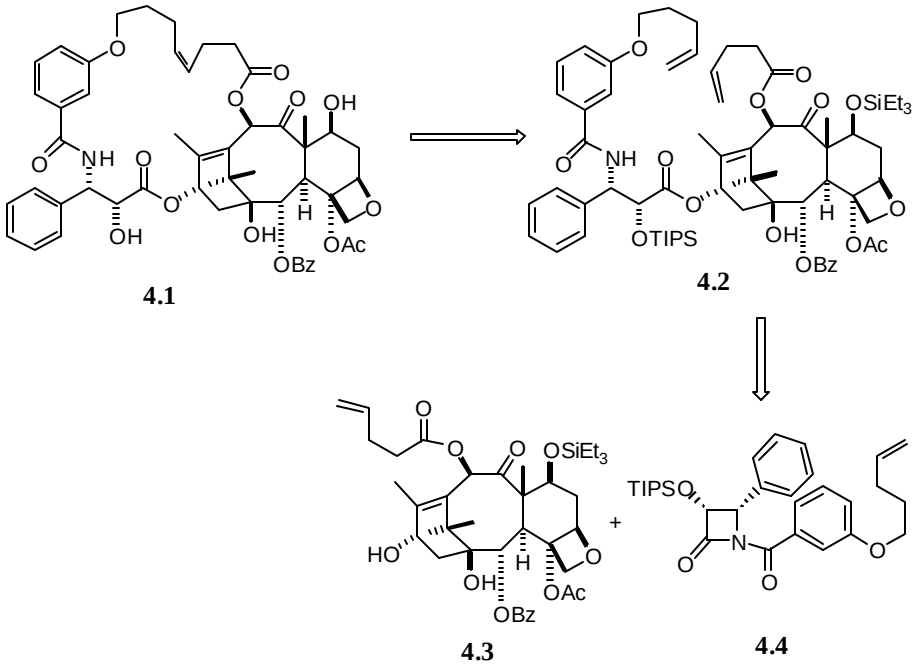

Scheme 4.1 Retrosynthesis analysis of macrocyclic taxoid **4.1**

Retrosynthetic analysis of macrocyclic analogs in Scheme 4.1 shows that the synthesis of macrocyclic analog **4.1** can be achieved by a ring–closing olefin metathesis

of taxoid–ù,ù′–diene **4.2**. Compound **4.2** could be synthesized from 10–deacetylbaccatin and β–lactam compound **4.4**.

The synthesis of the baccatin core began from 10–deacetylbaccatin with initial acetylation and complete protection to afford compound **4.6** in 85% yield (Scheme 4.2). The removal of the acetate group at C–10 was followed by reacylation with 4-pentenoyl chloride gave **4.7** in 64% yield.

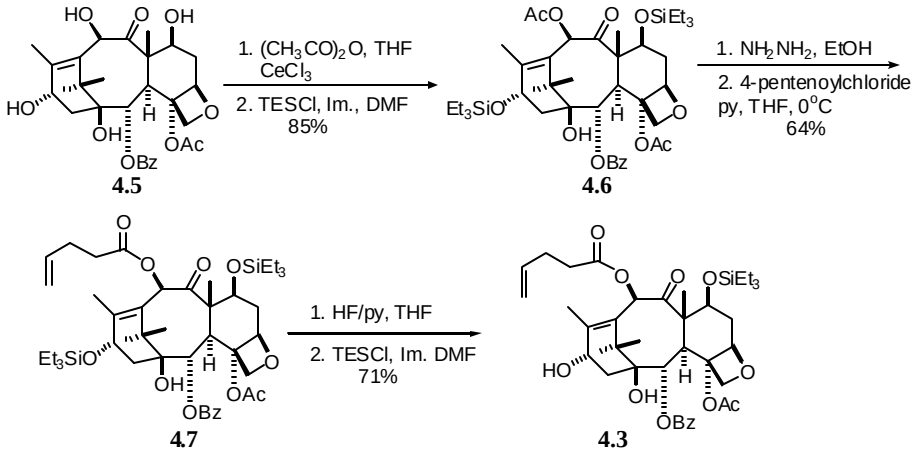

Scheme 4.2 Synthesis of compound **4.3**

Complete deprotection of the C–7 and C–13 triethylsilyl groups and selective reprotection of the C–7 group concluded the synthetic scheme to produce **4.3**. A more efficient two step route towards the same target compound (Scheme 4.3) was later adopted to synthesize the baccatin core and was optimized to give **4.3** in over 90 % overall yield for the two steps.

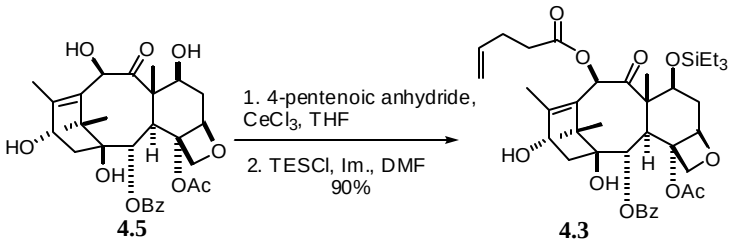

Scheme 4.3 Alternative synthesis of compound **4.3**

With the objective of diversifying the C–10 tethered macrocycle analogs, the synthesis of various β–lactams modified at the benzamide group was carried out by the

coupling of **4.8** with the respective acid chlorides containing a terminal olefin in the presence of a base and catalytic amount of DMAP. The products **4.4** and **4.9 – 4.12** were obtained in yields of 72–90% (Scheme 4.4).

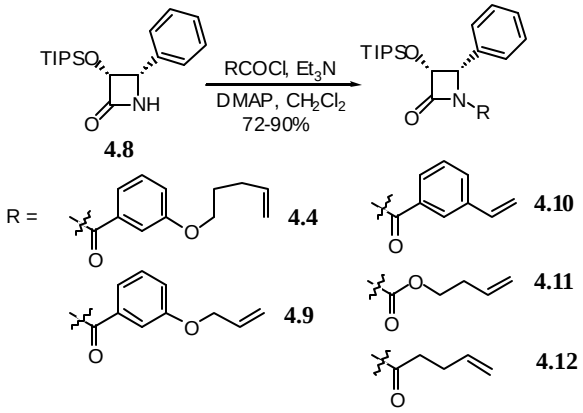

Scheme 4.4 Synthesis of β-lactams analogs

All β–lactams prepared according to Scheme 4.4 were coupled to the C–10 modified baccatin core **4.3** as shown in Scheme 4.5, and gave the respective substrates for ring–closing (**4.2, 4.13, 4.14, 4.15, 4.16**) in moderate yields.

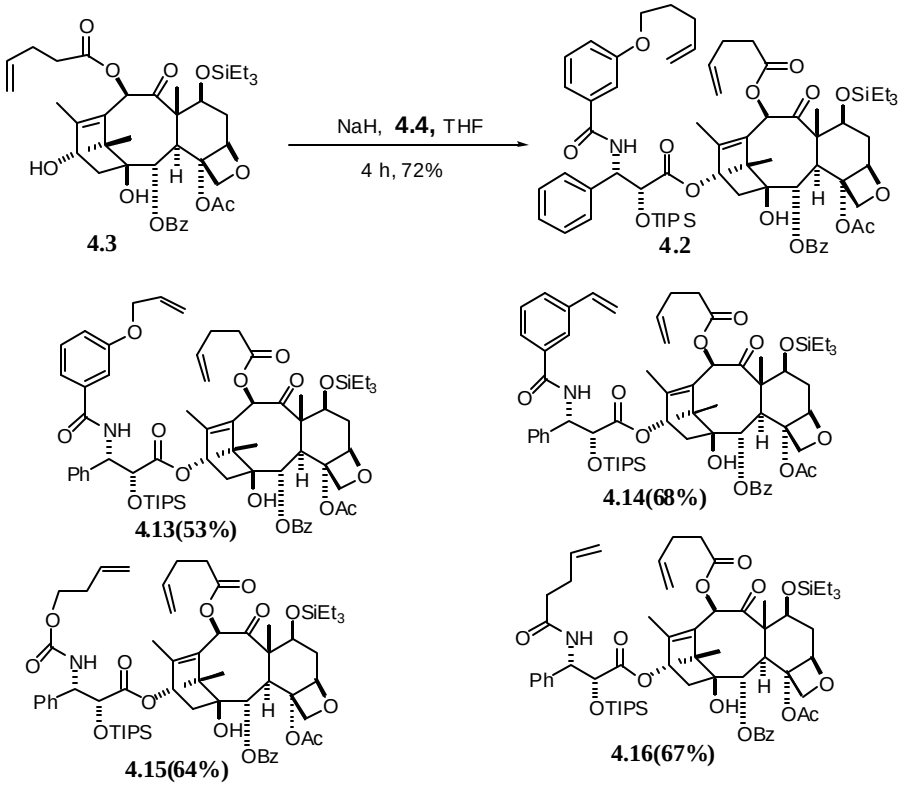

Scheme 4.5 Coupling reaction and coupled products

Macrocyclization of each of the coupled products was attempted with the second generation Grubbs catalyst and different reaction conditions. Cyclized product was obtained only for substrate **4.2** (Scheme 4.6); all other substrates produced mixtures of inseparable side products.

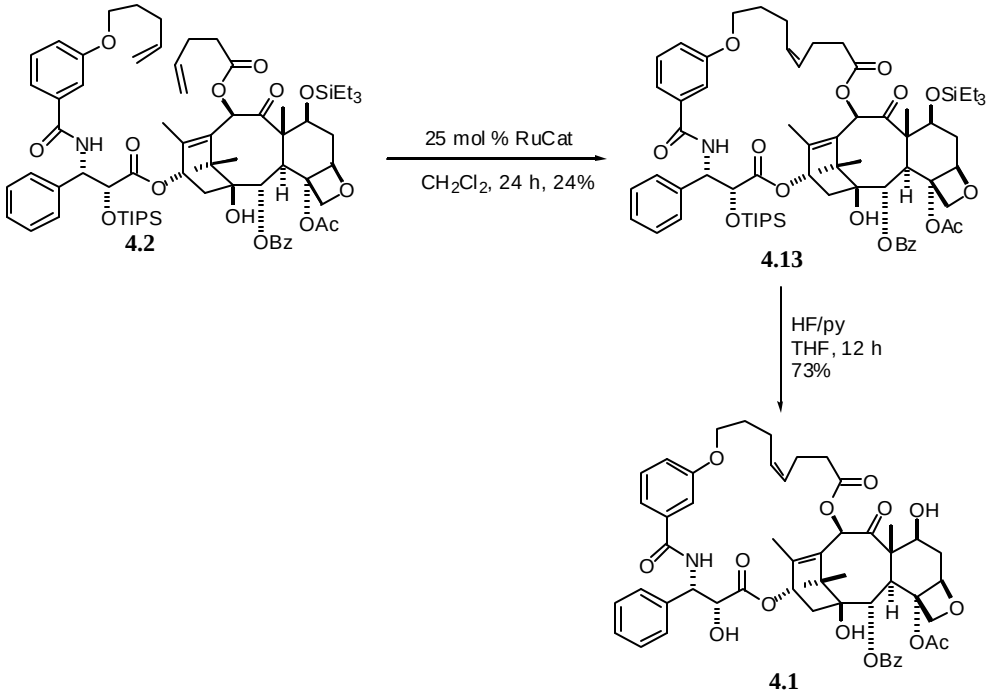

4.2 **4.13** **4.1**

Scheme 4.6 Synthesis of macrocyclic analog **4.1**

4.2 Bioactivity

The bioactivity results for macrocyclic analog **4.1** showed a 16–fold lesser activity than taxol in A2780 cytotoxicity assay. Moreover **4.1** exhibited a two–fold lesser activity as compared to the previously described macrocyclic analogs **3.3** and **3.4**. The lesser activity of the C–10 tethered macrocyclic analog might be due to the conformational changes caused by the tether, which totally removes the convex shape of the baccatin core of taxol. It is however essential to perform conformational analysis in order to identify the actual conformational changes introduced by the tether.

Table 4.1 Bioactivity Results (**4.1**)

Compound	Cytotoxicity to A2780 Mammalian cells (IC_{50}, mg/mL)
Taxol	0.32 ± 0.08
4.1	4.96 ± 1.12

In order to rationalize the weaker activities of the macrocyclic taxol analog, our collaborators (Snyder and co–workers) performed docking experiment with the best fit on T–taxol in β–tubulin. The results of the experiment indicated that, the hydrocarbon linker on the macrocycle is exposed to the aqueous (polar) medium, which could be responsible for inefficient binding on β–tubulin (Figure 4.1). Moreover, the solvation of polar substituents on C7–C10 is also deterred by the hydrophobic linker leading to poor binding.

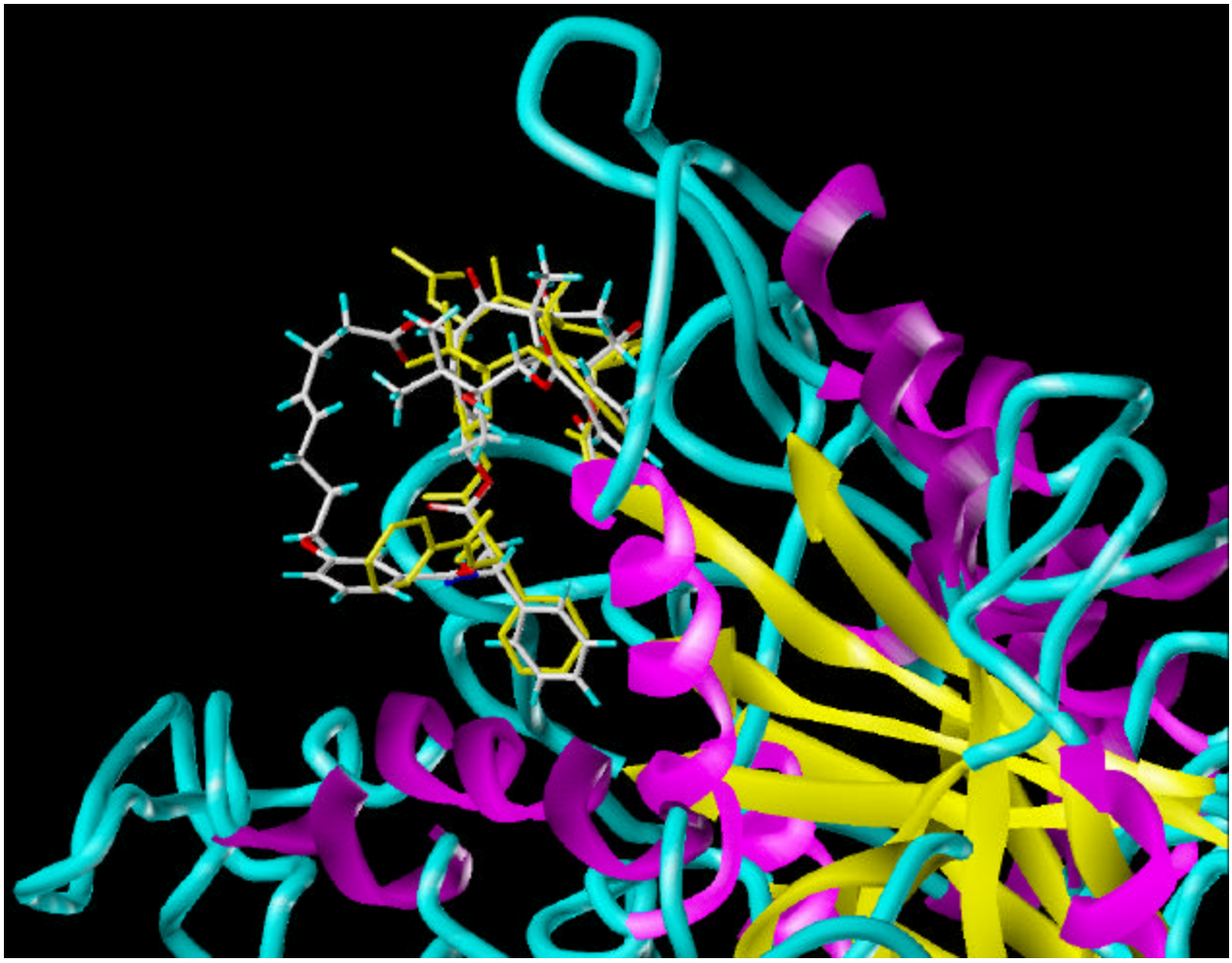

Figure 4.1 The C10–C3' bridged Taxol superimposed on T-Taxol (yellow) in β-tubulin. The largely hydrophobic bridge is exposed to the aqueous phase.

5. ATTEMPTED SYNTHESES OF CONFORMATIONALLY RESTRICTED SIDECHAINS

5.1 Background

Identifying the taxoid pharmacophore relies on the understanding of the active conformation of the natural product. In taxol, the baccatin core is conformationally rigid, however the flexibility of the sidechain resulted in about three major possible conformations.[53a,56,57] The existence of more than one possible conformation adds complexity to the identification of the biologically relevant conformation.[79] Hence, it become necessary to investigate analogs with conformationally restricted sidechain.

Barboni and coworkers synthesized and performed biological evaluation of taxol analogs possessing conformationally restricted sidechains (Figure 5.1).[95] Compound **5.2**

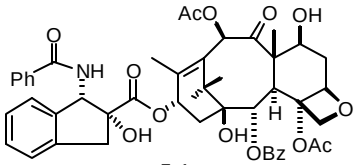

5.1

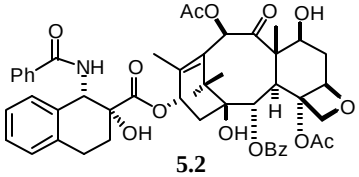

5.2

Figure 5.1 C2'-C3' restricted taxol analogs

was completely inactive both in tubulin–binding and cytotoxicity assays. Compound **5.1** showed a four–fold lesser activity than taxol in tubulin–binding assays and a nine–fold lesser activity than taxol in cytotoxicity (MCF7 cells) assays. According to the authors the observed activity means that there may be a taxoid family of conformers supporting a narrow range of H–C2'–C3'–Ph dihedral angles that are ideal for binding.

Our group proposed to synthesize taxol analogs with 3'–Ph and the benzamide phenyl groups fused together (**5.3**) or tethered with a linker to introduce a different conformational constraint on to the sidechain.

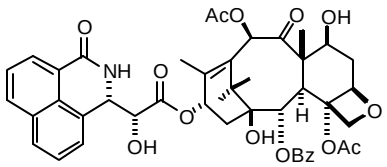

5.3

5.2 Attempted Syntheses Approaches

The synthesis of **5.3** was first envisioned by the coupling of a β–lactam sidechain (route **a**) or alternatively the acid (route **b**) with an appropriately protected baccatin core as shown in Scheme 5.1.

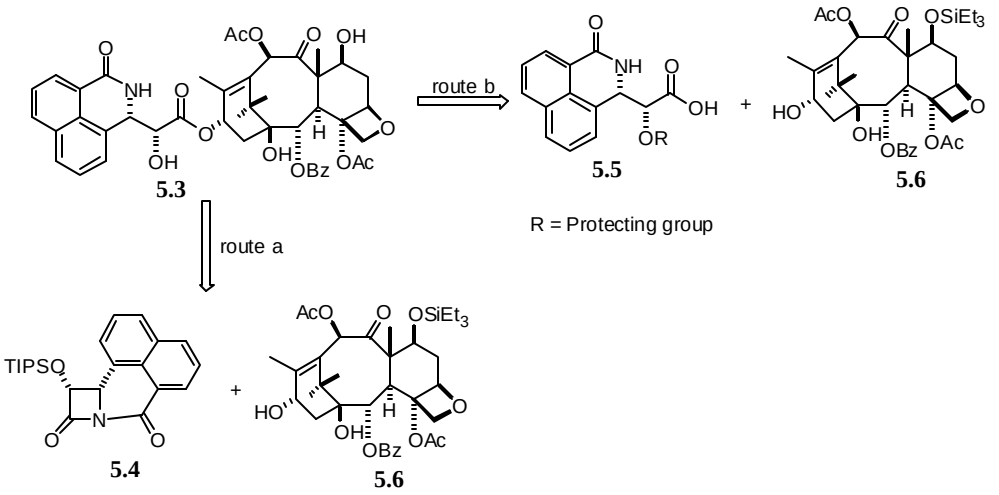

Scheme 5.1 Retrosynthetic analysis of **5.3**

Initially we adopted the synthesis of compound **5.3** *via* route **a** in the forward synthesis direction. The key element in the synthesis of the target compound is the preparation of **5.4**. Accordingly, the synthesis began with the reaction of commercially available 1,8–naphthalic anhydride with LAH to give the diol* in 72% yield (Scheme

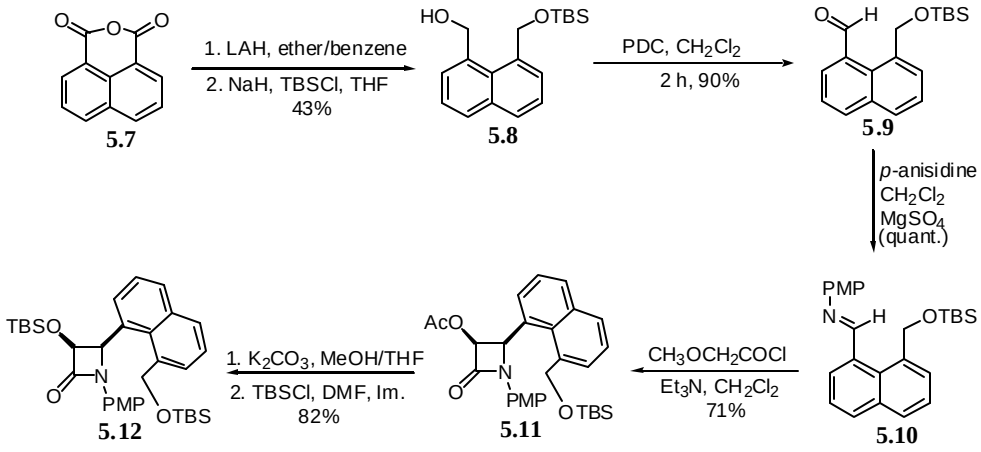

Scheme 5.2 Synthesis of fused sidechain

* Currently this chemical is available from Aldrich [Cat. No. 49,529–8 (1,8–Naphthalenedimethanol)]

5.2). Monoprotection of the diol as its *t*–butyldimethylsilyl ether **5.8** followed by oxidation of the primary alcohol to afforded **5.9** in 60% yield. The aldehyde was then condensed with *p*–anisidine to give the corresponding imine quantitatively. Reaction of the imine with acetoxyacetyl chloride produced the racemic β–lactam, which was then hydrolyzed and protected to give **5.12**. Functional group manipulations (three steps) gave the acid 5.13. Cyclization of **5.13** to the desired imide **5.4** was attempted using several different conditions. Unfortunately none of the conditions used gave any desired product, and this route was dropped.

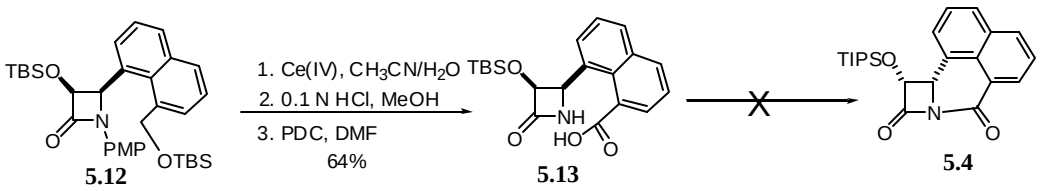

Scheme 5.3 Attempted synthesis of fused side chain **5.4**

The alternative approach (route **b**) was also investigated. In this route the main strategy was to introduce the *syn* amino and hydroxy functions by using the Sharpless aminohydroxylation procedure.[106] This strategy required the preparation of the *trans*–olefin compound **5.15** as a starting material (Scheme 5.4).

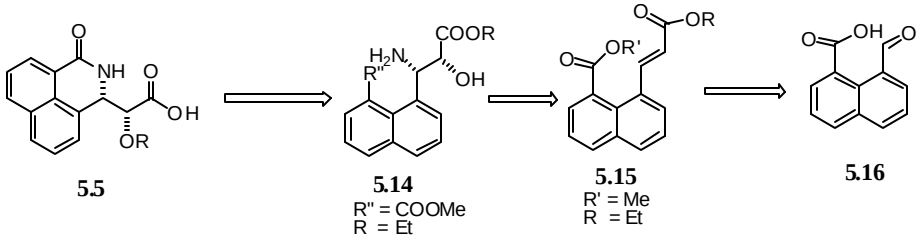

Scheme 5.4 Retrosynthesis analysis of **5.5**

The commercially available 1,8–naphthaldehydic acid was converted to its methyl ester and two carbon homologation by a Wittig reaction afforded the desired fluorescent *trans*–olefin (**5.15**) in 65% yield.

[106] Demko, Z. P; Bartsch, M.; Sharpless, K. B. *Org. Lett*. **2000**, *2*, 2221–2223.

Prior to the aminohydroxylation of the *trans*–olefin, the preparation of the nitrogen transfer agent *N*–bromo–chloroacetamide was accomplished by the reaction of *N*–chloroacetamide and a brominating agent DBI (dibromoisocyanuric acid)* following a reported procedure.

The aminohydroxylation reaction was carried at 0 ^{o}C for 24 h (Scheme 5.5). The characterstics deep greenish color of the dioxo osmium (VI) complex was observed after the addition of the *N*–bromo–chloroacetamide. After work–up the crude product showed the presence of a compound with no olefinic protons in the proton NMR spectra. Analysis of the crude mixture shwed that it contained partial and completely hydrolyzed ester groups, and dihydroxylated rather than aminohydroxylated products. The dihydroxylation reaction might be favored due to the steric hindrance of the ester group to the nitrogen–transfering agent (2–chloro–*N*–bromoacetamide).

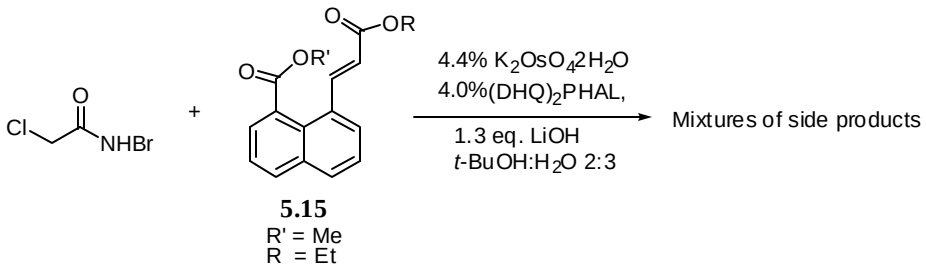

5.15
R' = Me
R = Et

Scheme 5.5 Aminohydroxylation reaction

Even though the single step aminohydroxylation reaction was attractive, and proved to be useful in the transformation of regular cinnamates, the complexity of our substrate made it a less applicable method towards our target.

Ring–closing olefin metathesis reaction of representative β–lactams (**5.16, 5.17, 5.18**) were also performed to synthesize conformationally constrained sidechain. Multiple reactions were run with variation of reaction conditions (as described in Table 3.3). However, none of the substrates gave a cyclized product, only traces of dimeric products were observed for substrates **5.17** and **5.18**.

* DBI was prepared by the reaction of cyanuric acid and bromine

The unsuccessful reactions led us to test the reactions once again with the sidechains formed after coupling the lactams to the baccatin core (Scheme 5.6). It was hoped that this route would relieve any strain during the cyclization and hoping to bring about a productive cyclization. Substrates (**5.19, 5.20, 5.21**) were prepared and subjected

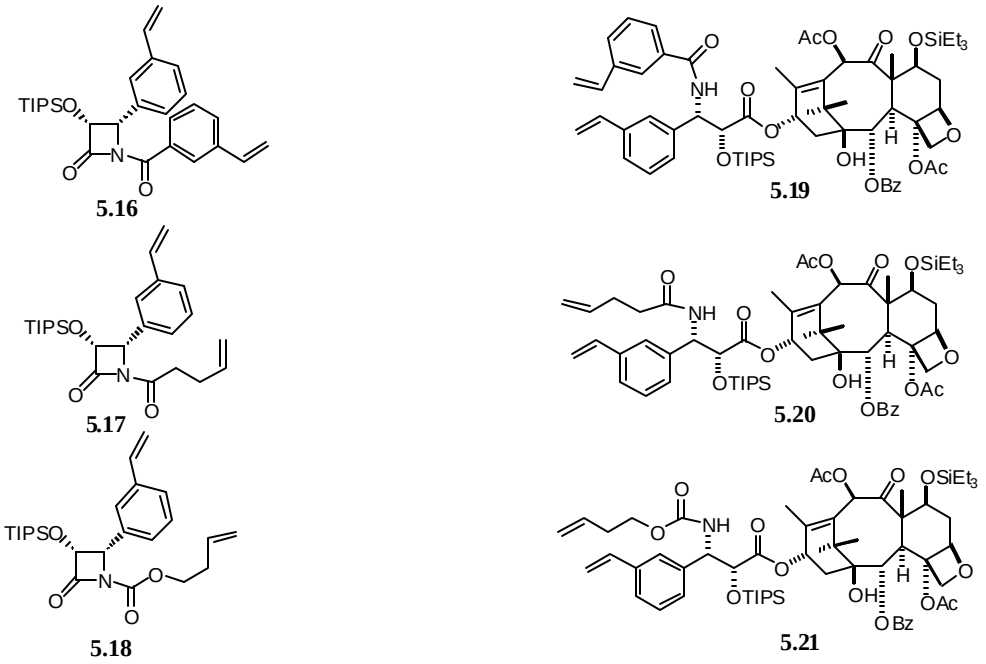

Scheme 5.6 Substrates tested for ring-closing olefin metathesis

to RCM reaction conditions, however none of the reactions gave fruitful cyclizations.

Heck–coupling of **5.22** and the ring opened methyl ester sidechain **5.23** was also sought as a strategy to get the cyclized product (Scheme 5.7). The reactions were attempted in acetonitrile and DMF, and did not give the cyclized product.

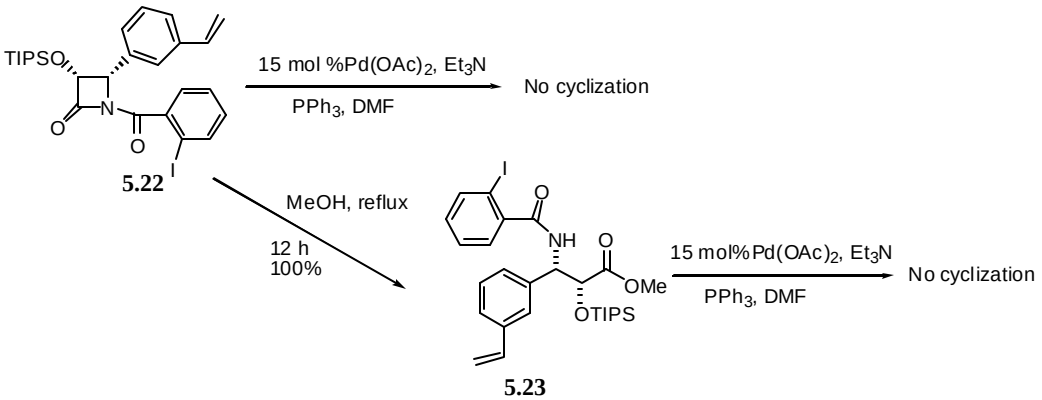

Scheme 5.7 Attempted palladium catalyzed cyclization

6. CONCLUSIONS

The synthesis of a triply labeled taxol analog for REDOR NMR experiments has been accomplished. The labeling pattern at the 3'–phenyl (D–Ph), 4–OAc (CD_3CO) and the 2–benzoate (F–Ph) represents both the sidechain and the baccatin core. The result of the REDOR NMR is experiment is expected to give important internuclear distances of the tubulin–bound taxol. These internuclear distances can be compared to the existing taxol conformation and will contribute in the understanding and identification of the biologically active conformation of taxol.

The synthesis of two macrocyclic analogs **3.3** and **3.4** tethered from the 3'-Ph to the C–4 acetate group was achieved by a ring–closing olefin metathesis. Their biological assays indicated an approximately tenfold weaker activity as compared to taxol both in the cytotoxicity and tubulin polymerization assays. Computational analysis and docking experiments on these analogs showed that their conformational candidates included conformations similar to T–taxol. Docking experiments of the analogs on tubulin showed that residue Phe^{272} of tubulin interfered with the propene unit of the linker, suggesting that shorter linkers probably would have improved activity.

The macrocyclic analog (**4.1**) with a tether from the C–10 to the benzamido group on the sidechain also showed a forty–fold lesser activity than taxol in the A2780 cytotoxicity assay. The weak bioactivity of this analog was rationalized based on the docking experiment to tubulin, which showed that the hydrophobic linker sits out into the polar medium in the binding region, leading to inefficient binding.

The screening of analogs with comparable or better activity than taxol requires the synthesis of libraries of several macrocyclic analogs, but in this study we encountered problems in the crucial macrocyclization reactions by ring–closing olefin metathesis. The problems were the production of inseparable complex mixtures, the lack of any product formation product formation even up to 50 mol% catayst loading, and removal of the ruthenium catalyst after the reaction. These problems are current issues in the development of highly stable, active, and polymer supported ruthenium catalysts.

Future research plans could focus on the utilization of other macrocyclization strategies. The most viable alternative would be the application of macrolactonization with an appropriately functionalized sidechain and baccatin core.